PHYSICAL REVIEW A, VOLUME 63, 010702(R)

Inner-shell photoabsorption of Fe^{14+}: Unimportance of correlation and relativistic effects

T. W. Gorczyca,[1] Z. Felfli,[2] N. C. Deb,[3] and A. Z. Msezane[2]
[1]*Department of Physics, Western Michigan University, Kalamazoo, Michigan 49008*
[2]*Center for Theoretical Studies of Physical Systems, Clark Atlanta University, Atlanta, Georgia 30314*
[3]*Department of Applied Mathematics and Theoretical Physics, The Queen's University of Belfast, Belfast BT7 1NN, United Kingdom*
(Received 1 August 2000; published 30 November 2000)

We have performed a series of calculations of the photoabsorption cross section of Fe^{14+} near the $2p^{-1}$ and $2s^{-1}$ edges, within the framework of *R*-matrix theory. We find the unexpected result that the inclusion in the calculation of such effects as the spin-orbit interaction and higher-order correlations leads to a mere redistribution of flux among the various final channels, while the total *convoluted* photoabsorption cross section remains virtually unchanged. Hence, an appropriate minimal configuration *LS* coupling representation can adequately describe inner-shell *total* photoabsorption cross sections, leading to a saving in computational effort by orders of magnitude compared to more elaborate calculations.

DOI: 10.1103/PhysRevA.63.010702 PACS number(s): 32.80.Fb, 32.80.Hd

Photoionization of multiply charged ions near their inner-shell thresholds is an important field of study, particularly for systems that are crucial to the investigation of stellar atmospheres [1,2] and the modeling of laboratory plasmas [3,4], such as the iron ions. Most of the available studies of iron ions to date have dealt almost exclusively with outer-shell excitation and ionization. This is due in part to processor power and, to a lesser extent, memory and storage limitations. The multiple open shell nature of inner-shell processes, and the larger magnitude of the spin-orbit operator for inner-shell excited highly charged ions, would suggest the need for a highly correlated, relativistic theoretical approach, and indeed recent studies have considered this to some extent for the case of Fe^{14+} photoionization [5,6].

The initial motivation of the present paper was to confirm, for Fe^{14+}, our previous findings for photoionization of Ne [7] and Ne-like iron [8], where we established that relativistic effects can be efficiently taken into account within the framework of *LS*-coupled *R*-matrix theory, and without having to resort to extensive fully or semirelativistic calculations, such as Dirac or Breit-Pauli *R*-matrix methods. The idea is to combine an *LS R*-matrix calculation with an intermediate coupling *LS-JK* frame transformation using multichannel quantum defect theory (MQDT) and computed term coupling coefficients, as was described in our earlier work on Ne [7]. The Fe^{15+} final ionic states are described by a highly converged configuration-interaction (CI) basis (a full Breit-Pauli calculation would have been too memory intensive for the available computer resources).

Unexpectedly, we found that even the simplest *R*-matrix calculation, including only the minimal CI representation of the Fe^{15+} targets, and neglecting relativistic effects, reproduced the energy-averaged results from the more elaborate, highly correlated, *LS-JK* frame transformation calculation. We discuss this below as being due to a redistribution of oscillator strengths among the final channels, leaving the sum essentially unaltered. We first describe the problem, then briefly detail the various sets of calculations, comparing both detailed and energy-averaged results of the various levels of calculations, and finally discuss their implications.

In the lowest-order treatment, the following photoabsorption processes are possible near the *L*-shell edge of Fe^{14+}:

$$h\nu + 2s^2 2p^6 3s^2 \rightarrow \left\{ \begin{array}{l} 2s^2 2p^5 3s^2 kl' \\ 2s 2p^6 3s^2 kl'' \end{array} \right\}$$

$$\rightarrow 2s^2 2p^6 3s + e^-, \qquad (1)$$

$$\rightarrow 2s^2 2p^6 kl' + e^-. \qquad (2)$$

Here k denotes a bound electron n below threshold, and a continuum electron ϵ above threshold. The first of these decay paths in Eq. (1) is known as participator decay, and is accounted for by including the $2s^2 2p^6 3s$ target state of Fe^{15+} in the close-coupling expansion, whereas the spectator decay represented by Eq. (2) (for $k=n$ only, below threshold) is accounted for with an optical potential [9]; the decay width of the latter is independent of n, so that the resonance profiles converging to each inner-shell threshold smoothly blend into the above-threshold ionization cross section. Intermediate states can be included via the inner-shell excited Fe^{15+} target states $2s^2 2p^5 3s^2$ and $2s 2p^6 3s^2$.

With this lowest-order treatment in mind, we first performed three sets of *R*-matrix calculations: (1) *LS*, (2) Breit-Pauli, and (3) *LS-JK* frame transformation. All *R*-matrix calculations utilized the Belfast suite of codes [10,11], and the frame transformation method [12,13] included an additional code developed initially for the treatment of relativistic effects in Ne [7] and Ne-like iron [8]. For the *N*-electron description of the Fe^{15+} target states, the $2s^2 2p^6 3s$,

TABLE I. Fe^{14+} and Fe^{15+} energies from the minimal-configuration basis.

		Absolute (a.u.)	$h\nu$ (eV)
Fe^{14+}	$2s^2 2p^6 3s^2\ ^1S_0$	−1182.982	0.00
Fe^{15+}	$2s^2 2p^6 3s\ ^2S$	−1166.092	459.61
Fe^{15+}	$2s^2 2p^5 3s^2\ ^2P^o$	−1139.408	1185.74
Fe^{15+}	$2s 2p^6 3s^2\ ^2S$	−1134.559	1317.68

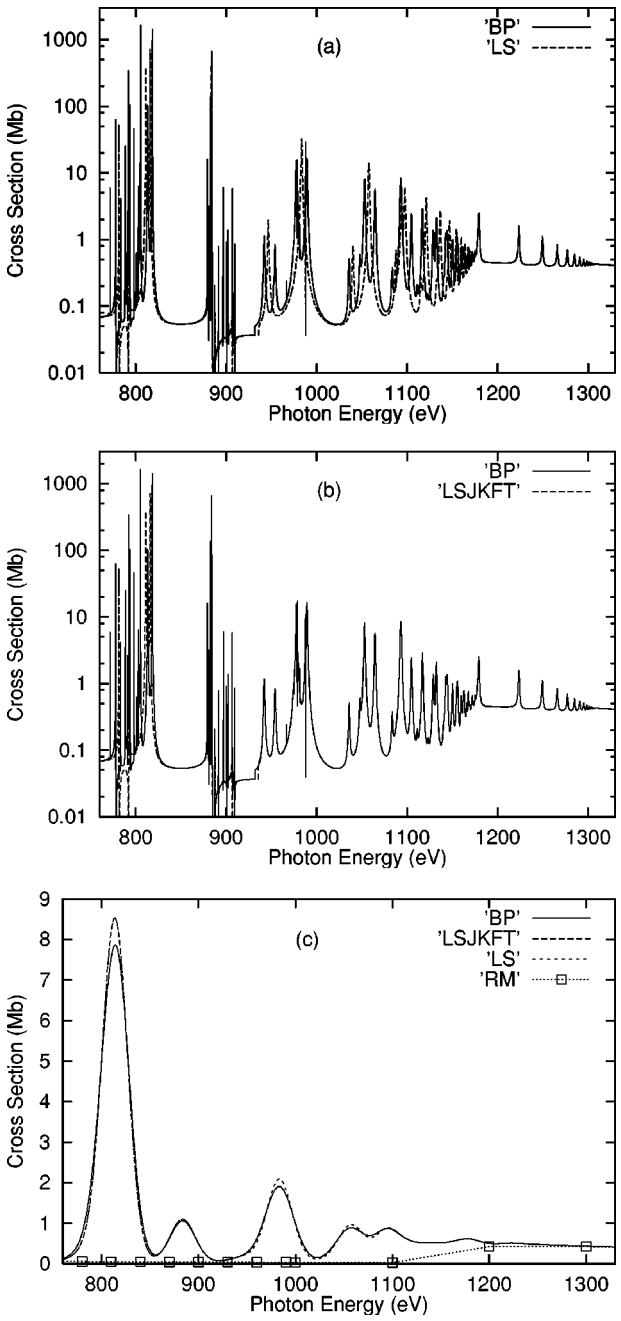

FIG. 1. Photoabsorption cross sections of Fe^{14+} using the minimal-configuration basis description. Comparisons between (a) Breit-Pauli (solid line) and LS (dashed line) results, (b) Breit-Pauli (solid line) and LS-JK frame transformation (dashed line) results, and (c) all three, convoluted with a 30-eV FWHM Gaussian. The independent-particle results of Reilman and Manson (RM) are also shown.

$2s^22p^53s^2$, and $2s2p^63s^2$ configurations were used. Configurations consistent with single and double promotions out of the $2s^22p^63s^2$ ground state were used for the corresponding $(N+1)$-electron states of Fe^{14+}, and the orbitals were generated from a Hartree-Fock [14] calculation on the $1s^22s^22p^63s$ ground state configuration of Fe^{15+}. Resultant energies are given in Table I.

Computed cross sections from this minimal configuration basis are presented in Fig. 1, all preconvoluted [15] with a 1-Ry Lorentzian in order to allow for a better resolution of the resonance strengths that become narrower near threshold. By comparing the full Breit-Pauli to the LS results in Fig. 1(a), it is seen that the semirelativistic effects included in the former cause a splitting of the $2s^22p^53s^2ns,md$ resonance series due to the 12-eV fine-structure splitting between the $^2P_{3/2}$ and $^2P_{1/2}$ parent levels. Otherwise, the overall resonance strengths appear to be the same. In Fig. 1(b), the results from an LS-JK Frame Transformation are seen to be quite similar, on this scale, to the Breit-Pauli ones except for the lowest-lying members of the $2s^22p^53s^2ns,md$ series; only for these lowest members, which reside in the R-matrix ''box,'' have fine-structure effects not been taken into account through the frame transformation [7,8]. The discrepancies are mostly due to slightly different resonance positions in the two results, causing relative differences in the cross section that oscillate about zero; even so, for the higher-lying resonances in the energy region $h\nu \geqslant 1000$ eV, we found that the maximum absolute difference was 5% or less. When energy averaged with a 30 eV full width at half maximum (FWHM) Gaussian, all three give essentially the same cross section due to the asymmetric nature of the cross-section differences [Fig. 1(c)]; semirelativistic interactions have little effect on the energy-averaged cross sections, and merely cause a splitting of resonance series. Above the $2s^{-1}$ threshold, all three agree with the earlier independent particle (IP)

TABLE II. Fe^{15+} radial orbitals.

Orbital	Slater-type coefficient	Power of r	Exponent
$1s$	252.938 863 4	1	26.037 500 0
	7.404 057 0	1	42.105 300 0
	0.336 703 6	2	10.380 100 0
	123.448 050 9	2	22.618 500 0
$2s$	−79.897 653 5	1	26.037 500 0
	−0.092 893 4	1	42.105 300 0
	459.718 259 8	2	10.380 100 0
	−464.663 628 0	2	22.618 500 0
$3s$	36.703 601 8	1	19.289 365 0
	−0.624 646 3	1	3.376 331 5
	−185.818 376 4	2	11.177 182 4
	−42.593 220 2	2	7.994 158 6
	325.268 003 6	3	5.967 604 0
	−419.816 159 3	3	9.459 865 7
$2p$	217.232 095 5	2	10.646 700 0
	187.119 067 7	2	16.723 400 0
	117.296 081 9	2	9.464 850 0
	11.918 031 9	2	36.874 900 0
$3p$	249.670 557 0	2	10.787 757 9
	−204.121 789 4	3	5.631 877 2
$3d$	177.434 212 1	3	5.719 955 5
	135.147 721 4	3	10.654 313 2

TABLE III. Fe^{14+} and Fe^{15+} energies from the highly correlated basis.

			Absolute (a.u.)	$h\nu$ (eV)
Fe^{14+}	$2s^2 2p^6 3s^2$	$^1S_0$	−1182.999	0.00
Fe^{15+}	$2s^2 2p^6 3s$	$^2S^e$	−1166.120	459.34
Fe^{15+}	$2s^2 2p^6 3p$	$^2P^o$	−1164.759	496.37
Fe^{15+}	$2s^2 2p^6 3d$	$^2D^e$	−1162.989	544.52
Fe^{15+}	$2s^2 2p^5 3s^2$	$^2P^o$	−1139.582	1181.46
Fe^{15+}	$2s^2 2p^5 3s 3p$	$^2D^e$	−1138.445	1212.40
Fe^{15+}	$2s^2 2p^5 3s 3p$	$^2P^e$	−1138.408	1213.41
Fe^{15+}	$2s^2 2p^5 3s 3p$	$^2S^e$	−1138.379	1214.22
Fe^{15+}	$2s^2 2p^5 3s 3p$	$^2D^e$	−1138.043	1223.34
Fe^{15+}	$2s^2 2p^5 3s 3p$	$^2P^e$	−1137.954	1225.77
Fe^{15+}	$2s^2 2p^5 3s 3p$	$^2S^e$	−1137.521	1237.54
Fe^{15+}	$2s^2 2p^5 3s 3d$	$^2P^o$	−1137.260	1244.67
Fe^{15+}	$2s^2 2p^5 3s 3d$	$^2F^o$	−1137.154	1247.53
Fe^{15+}	$2s^2 2p^5 3s 3d$	$^2D^o$	−1137.049	1250.40
Fe^{15+}	$2s^2 2p^5 3s 3d$	$^2D^o$	−1136.973	1252.45
Fe^{15+}	$2s^2 2p^5 3s 3d$	$^2P^o$	−1136.698	1259.95
Fe^{15+}	$2s^2 2p^5 3s 3d$	$^2F^o$	−1136.562	1263.66
Fe^{15+}	$2s 2p^6 3s^2$	$^2S^e$	−1134.688	1314.63
Fe^{15+}	$2s 2p^6 3s 3p$	$^2P^o$	−1132.992	1360.79
Fe^{15+}	$2s 2p^6 3s 3p$	$^2P^o$	−1132.841	1364.90
Fe^{15+}	$2s 2p^6 3s 3d$	$^2D^e$	−1132.268	1380.49
Fe^{15+}	$2s 2p^6 3s 3d$	$^2D^e$	−1131.578	1399.28

results of Reilman and Manson [16], validating their results above threshold. Clearly, the inner-shell resonances, which are not taken into account in the Reilman and Manson results, are a dominant contribution to the cross section below the $2p^{-1}$ and $2s^{-1}$ thresholds.

We next consider the effects of higher-order correlations. A target wave function, now including the $3p$ and $3d$ orbitals, was generated using the program CIV3 [17] with the Clementi and Roetti [18] orbitals as input to describe N-electron configurations consistent with single and double promotions out of the $2s^2 2p^6 3s$, $2s^2 2p^5 3s^2$, and $2s 2p^6 3s^2$ configurations. The $3p$ and $3d$ orbitals were optimized on the energies of the $2s^2 2p^6 3p\ ^2P^o$ and $2s^2 2p^6 3d\ ^2D$ levels, respectively. The parameters of the radial orbitals of the target wave function are given in Table II. In addition to the usual electron-electron Hamiltonian, relativistic effects, namely the spin-orbit, spin-other-orbit, spin-spin, mass correction, and Darwin terms, were included. The diagonal elements of the Hamiltonian matrix were adjusted slightly to reproduce the experimental energies [19] as close as possible. Each radial function is a sum of Slater-type orbitals; the square of each orbital, integrated from 0 to ∞, is unity. Resultant energies of this larger calculation, which include all CI states that differ from the minimal configuration description by at most one electron, are given in Table III. For the $(N+1)$-electron description, all configurations consistent with single, double, and triple promotions out of the $2s^2 2p^6 3s^2$ ground-state configuration were used.

Results from this more extensive calculation are shown in Fig. 2, using both LS and LS-JK frame transformation methods; a full Breit-Pauli calculation using this basis would have been too memory-intensive for the available computational facilities (see, for instance, Refs. [7] and [8]). Again it is seen that, apart from the fine-structure splitting of the $2p^{-1}_{3/2}$ and $2p^{-1}_{1/2}$ series, the nonrelativistic and semirelativistic results are essentially the same. Finally, we compare in Fig. 3 the energy-averaged results from both the minimal-configuration LS calculation and the more complex CI LS-JK frame transformation calculation. It can be seen that these two methods give essentially the same cross section; however, the former required a four-channel close-coupling expansion and took less than a minute of CPU time to compute the 100 000 energy points used, whereas the latter required 102 channels and took more than two days.

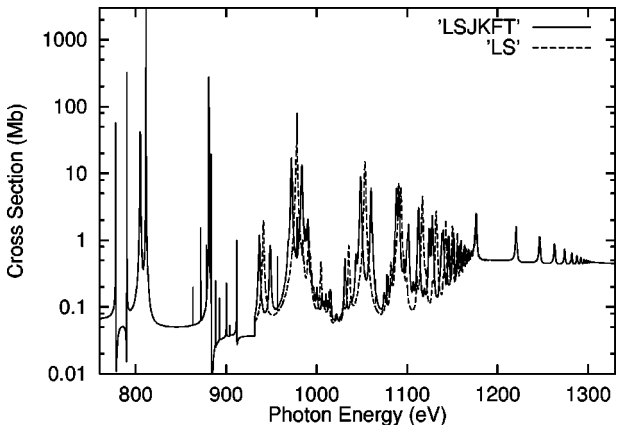

FIG. 2. Comparison between LS-JK frame transformation (solid line) using the highly correlated configuration basis description and LS (dashed line) photoabsorption cross sections of Fe^{14+}.

We now consider the actual effect of CI and/or the spin-orbit interaction on the computation of total photoabsorption cross sections. These can be expressed as

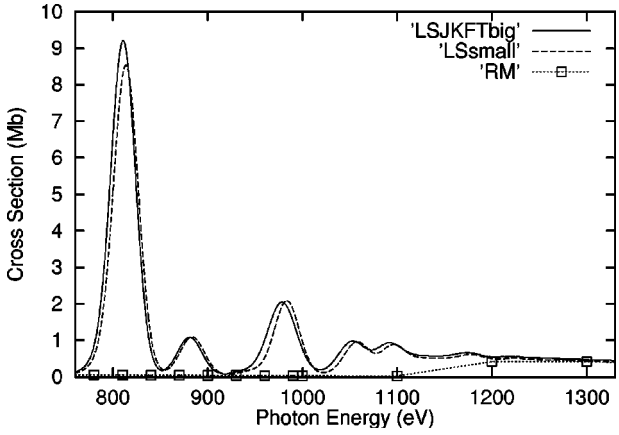

FIG. 3. Comparison between the LS-JK frame transformation (solid line) photoabsorption cross sections of Fe^{14+} using the highly correlated basis and the LS results (dashed line) using the minimal-configuration description, both convoluted with a 30-eV FWHM Gaussian. The former took more than two days of CPU time to complete the MQDT outer-region calculation for 100 000 energy points, whereas the latter took less than 1 min. The Reilman and Manson (RM) results are also shown.

$$\sigma_{total} = \frac{4\pi^2\omega}{3c} \sum_i \langle \Psi_i | D | \Psi_0 \rangle \langle \Psi_0 | D | \Psi_i \rangle, \qquad (3)$$

where ω is the photon energy, Ψ_0 denotes the initial wave function of the $2s^2 2p^6 3s^2 (^1S_0)$ ground state, and Ψ_i is the wave function for each of the final continua (including embedded resonances). The principal effect of introducing additional CI wave functions, or the spin-orbit operator into the Hamiltonian, is to mix, or rotate, the various final wave functions Ψ_i. However, this orthogonal transformation does not affect the *total* sum given in Eq. (3). Hence, these effects, while certainly important for individual *partial* cross sections [each of the separate terms in the sum of Eq. (3)], are unimportant for *total* cross sections.

In conclusion, we have found that a minimal configuration basis description, guided by independent-particle considerations, is sufficient for calculating the total inner-shell photoabsorption cross section of Fe^{14+}, even though the high charge would suggest that relativistic effects should be important, and the open shell nature would suggest the importance of higher correlations. These results also confirm the above-threshold IP results of Reilman and Manson [16], although here we have also included the dominating contributions from inner-shell excited resonances, which are important for accurately modeling astrophysical plasmas.

ACKNOWLEDGMENTS

T.W.G. was supported in part by NASA Grant No. NAG5-9581. Work at Clark Atlanta U. was supported by the U.S. Department of Energy, Office of Basic Energy Science, Division of Chemical Science under Contract No. DE-FG05-84ER13266. N.C.D. is currently supported by EPSRC of the UK.

[1] H.E. Mason and B.C. Monsignori-Fossi, Astron. Astrophys. Rev. **6**, 123 (1994).
[2] G. J. Ferland and D. A. Verner, in *Atomic Processes in Plasmas*, edited by E. Oks and M. S. Pindzola (AIP, Woodbury, NY, 1998), pp. 163-172, and references therein.
[3] H.P. Summers, Adv. At., Mol., Opt. Phys. **33**, 275 (1994).
[4] J. L. Terry, B. Lipschultz, A. Yu. Piragov, C. Boswell, S. I. Kasheninnikov, B. LaBombard, and D. A. Pappas, in *Atomic Processes in Plasmas*, edited by E. Oks and M. S. Pindzola (AIP, Woodbury, NY, 1998), pp. 43–57, and references therein.
[5] N. Haque and A.K. Pradhan, Phys. Rev. A **60**, R4221 (1999).
[6] M.A. Bautista, J. Phys. B **33**, L419 (2000).
[7] T.W. Gorczyca, Z. Felfli, H.-L. Zhou, and S.T. Manson, Phys. Rev. A **58**, 3661 (1998).
[8] N. Haque, H.S. Chakraborty, P.C. Deshmukh, S.T. Manson, A.Z. Msezane, N.C. Deb, Z. Felfli, and T.W. Gorczyca, Phys. Rev. A **60**, 4577 (1999).
[9] T.W. Gorczyca and F. Robicheaux, Phys. Rev. A **60**, 1216 (1999).
[10] P. G. Burke and K. A. Berrington, *Atomic and Molecular Processes: An R-matrix Approach* (IOP Publishing, Bristol, 1993).
[11] K.A. Berrington, W.B. Eissner, and P.H. Norrington, Comput. Phys. Commun. **92**, 290 (1995).
[12] U. Fano, Phys. Rev. A **2**, 353 (1970).
[13] M. Aymar, C.H. Greene, and E. Luc-Koenig, Rev. Mod. Phys. **68**, 1015 (1996).
[14] C. Froese Fischer, Comput. Phys. Commun. **64**, 369 (1991).
[15] F. Robicheaux, Phys. Rev. A **48**, 4162 (1993).
[16] R.F. Reilman and S.T. Manson, Astrophys. J., Suppl. Ser. **40**, 815 (1979).
[17] A. Hibbert, Comput. Phys. Commun. **9**, 141 (1975).
[18] E. Clementi and C. Roetti, At. Data Nucl. Data Tables **14**, 177 (1974).
[19] J. Sugar and C. Corliss, J. Phys. Chem. Ref. Data Suppl. 2 **14**, 473 (1985).